7-2006

Field-Induced Polymer Wall Formation in a Bistable Smectic-A Liquid Crystal Display

Ebru A. Buyuktanir
Kent State University - Kent Campus

Nadina Gheorghiu
Kent State University - Kent Campus

John L. West
Kent State University - Kent Campus, jlwest@kent.edu

Maxim Mitrokhin
TechnoDisplay AS

Borre Holter
TechnoDisplay AS

See next page for additional authors

Field-induced polymer wall formation in a bistable smectic-A liquid crystal display

Ebru A. Büyüktanir,[a] Nadina Gheorghiu, and John L. West
Liquid Crystal Institute, Kent State University, Kent, Ohio 44242

Maxim Mitrokhin and Børre Holter
TechnoDisplay AS, Ynglingeveien 42, P.O. Box 2, N-3184 Horten, Norway

Anatoliy Glushchenko
University of Colorado at Colorado Springs, 1420 Austin Bluffs, Colorado Springs, Colorado 80933

(Received 27 April 2006; accepted 10 June 2006; published online 17 July 2006)

We developed a composite system to produce robust bistable smectic-A (SmA) liquid crystal based flexible displays by encapsulating the liquid crystal material in a polymer wall structure. While keeping all the intrinsic bistable properties of the SmA material, the field-induced polymer walls bridge the two display substrates and bring significant advantages over the polymer dispersed liquid crystal structure. Here we analyze the performance of an encapsulated pixel and demonstrate superior electro-optical characteristics, high contrast ratio, and excellent sunlight readability.
 [DOI: 10.1063/1.2221887]

Bistable liquid crystal (LC) devices[1–3] have generated great interest among researchers because of their unique electro-optic properties, mainly their ability to maintain an image indefinitely without power consumption, promising many unique display applications. Recently, more research efforts have been devoted to producing bistable LC display technology on plastic substrates rather than on glass substrates for potential use in several flexible display applications.[4–6] The possibility of preparing flexible liquid crystal films on plastic substrates is challenging because of the difficulty of maintaining a uniform thickness and preventing air bubble-free formation after their mechanical bending. Consequently, the addition of polymer network infrastructure is required to provide mechanical stability to the LC device.

One decade ago researchers reported a bistable display utilizing an ion-doped smectic-A (SmA) LC.[7,8] Ion-doped SmA LC devices retain two electrically switchable zero field stable optical states: (1) a transparent homeotropic state generated through dielectric reorientation of molecules at high frequency (>1 kHz) electric fields and (2) a scattering focal conic state generated through electrohydrodynamic instability (EHDI) at low frequency (<1 kHz) fields. The formation of intermediate scattering levels or the ratio of the pixel areas in homeotropic and in saturated focal conic states allows one to produce a large range of gray scale capability.[9] Since bistable SmA LC devices do not require polarizers or backlights, they are quite energy efficient when compared to the Twisted Nematic (TN) or Super Twisted Nematic (STN) displays. They can also maintain high contrast and wide viewing angles. Additionally, high resolution images can be produced using simple multiplex drive schemes.

Recently, we reported[10] development of a flexible plastic display by combining the idea of a polymer dispersed liquid crystal (PDLC) structure[11] with the use of bistable SmA materials. The polymer structure connects the two substrates providing with the display a necessary mechanical strength.[4,12] However, light scattering from numerous LC/polymer interfaces results in a decrease of the device contrast ratio (CR).

In our work, we report the development of the bistable SmA LC device incorporating polymer wall technology. The patterned field-induced polymer walls around pixels significantly improve CR for the SmA devices. In this case, the presence of the polymer does not deteriorate the performance of the smectic LC device, but provides an excellent pressure resistance and prevents a distortion of a display image. We show that the CR of the SmA LC encapsulated between polymer walls is much greater than that of the SmA PDLC system, approaching the CR value of the pure SmA material.

Polymer walls have been obtained by combining the effect of an applied electric field with the difference in the dielectric constants of the LC and monomer. In this case, the LC molecules diffuse to the high electric field pixel regions and the monomer to the low electric field interpixel regions.[13] The separation of the LC and monomer is due to the Kelvin polarization force,[14] of which the density is given by

$$\mathbf{F} = \mathbf{P} \cdot \nabla \mathbf{E}, \tag{1}$$

where $\mathbf{P}$ is the polarizability of the material and $\mathbf{E}$ is the electric field. The polarizability is related to the electric field

$$\mathbf{P} = (\varepsilon_d - \varepsilon_{\mathrm{mix}})\mathbf{E}, \tag{2}$$

where ε_d is the effective dielectric constant of the LC in the droplets, while $\varepsilon_{\mathrm{mix}}$ is the dielectric constant of the mixture with the monomer. Since the LC is aligned homeotropically by the strong electric field, ε_d is practically equal to $\varepsilon_{\parallel}$ of the LC. $\varepsilon_{\mathrm{mix}}$ is given by

$$\varepsilon_{\mathrm{mix}} = (\varepsilon_{\mathrm{LC}} - \varepsilon_m)c_{\mathrm{LC}} + \varepsilon_m, \tag{3}$$

where c_{LC} is the LC concentration and ε_m and $\varepsilon_{\mathrm{LC}}$ are the dielectric constants of the monomer and LC in the isotropic phase, respectively. From the center to the edges of the electrode region, the gradient in the electric field ranges from zero to its maximum value as does the Kelvin force. There-

[a]Electronic mail: buyuktan@lci.kent.edu

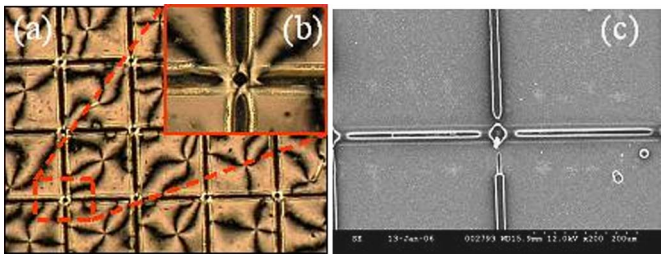

FIG. 1. (Color online) Transmission microscopy micrographs of the polymer walls produced in nematic LC by the patterned electric fields with (a) 5× and (b) 20× magnifications. (c) SEM picture of the polymer walls showing openings on the corners of the pixels.

fore, the phase separation is the most intense in the narrow interpixel region. Once formed, the LC droplets move from the interpixel to the pixel region, pushing the isotropic mixture towards the interpixel region, where the phase separation takes place. Subsequent UV exposure results in a polymer wall network enclosing the pixels occupied by the LC.

The ion-doped SmA LC used in this study was obtained from PolyDisplay ASA. This positive dielectric liquid crystal ($\Delta\varepsilon=8.75$) has the following phase transition temperatures: crystal ($T_{KA}=-5\ ^\circ$C)-SmA ($T_{AN}=52\ ^\circ$C)-nematic ($T_{NI}=59.7\ ^\circ$C)-isotropic. The polymer walls were formed using the mixtures of the photocurable material NOA65 from Norland Products Inc. and E44 LC from BDH Ltd. All the materials were used without further purification. The indium-tin-oxide (ITO) coated glass substrates were patterned by a photolithographic method. The widths of ITO lines and the spacing between them were 290 and 30 μm, respectively. Two patterned substrates were sandwiched to form a cell where the electrode lines were crossed. The cell thickness was controlled by the spherical Sekisui 16 μm thick spacers. The optimized SmA PDLC films[10] were prepared by means of polymerization-induced phase separation.

We observed that it is difficult to form polymer walls in the ionically doped SmA LC mixture. One of the reasons for this may be that the phase separation between the polymer and the LC was inhibited by the electrohydrodynamic turbulence. Therefore, to demonstrate the potential of the approach, polymer walls were formed in a mixture of nematic E44 LC ($\Delta\varepsilon=16.8$) and NOA65. Then the E44 LC was washed out and replaced with the ionically doped SmA material. After capillary filling of the nematic LC and NOA65 mixture at 110 °C, the cell was cooled down to room temperature at a rate of 0.3 °C/min while a square wave electric field with 1 kHz frequency and 12.8 V/μm amplitude was being applied to induce phase separation. Following that, the cell was irradiated with UV light for half an hour to fix the phase separated morphology. The transmission optical micrograph of the polymer walls in nematic LC is shown in Fig. 1. This template cell was immersed in hexane for one day, and later in tetrahydrofuran (THF) for 20 min to remove all of the nematic LC. Later, it was kept in vacuum chamber at 60 °C for 3 h to remove THF from the cell. After that the cell was refilled by ion-doped SmA LC material by vacuum-filling process above T_{NI} via the corner openings in each pixel, as seen in the detailed picture of the walls [Fig. 1(b)] and in the scanning electron microscopy (SEM) micrograph [Fig. 1(c)]. The corner openings of the walls are the result of the nonuniform electric fringing fields at the edges of the interpixel intersections.[13]

TABLE I. The summary of static-response measurements of SmA LC, SmA LC with polymer walls, and SmA PDLC at EHDI and FC-HT transition.

Frequency	SmA LC V_{th}	SmA LC V_{sat}	SmA with polymer walls V_{th}	SmA with polymer walls V_{sat}	SmA PDLC V_{th}	SmA PDLC V_{sat}
50 Hz	92	96	95	102	108	112
5 kHz	53	58	59	63	66	69

The electro-optical performances of all the SmA LC cells were measured in the normal transmission geometry at a 5° collection angle by using the 632.8 nm wavelength of a He–Ne laser. A 50 Hz square wave ac field was used to induce EHDI and transfer the cell from a transparent to opaque state. However, a 5 kHz ac field was applied to induce focal conic-homeotropic (FC-HT) transition.

Figure 2 shows the static-response characteristics of SmA LC, SmA LC with polymer walls, and SmA PDLC. The voltage was increased at a rate of 1 V s^{-1}. The threshold (V_{th}) and saturation (V_{sat}) voltages were tabulated in Table I for both transparent and opaque states. The response times and V_{sat} for FC-HT transition and EHD instability were determined at the 90% change in transmission when the cell was driven by an electric field, whereas V_{th} was determined at the 10% change in transmission.

In Fig. 3, the response times as a function of applied voltages were plotted by varying the applied voltages from 170 to 200 V for all three SmA LC cells at 5 kHz and 50 Hz frequencies. Comparing all the electro-optic results demonstrates that SmA LC cells with polymer walls perform very similar to pure SmA LC and much better than SmA PDLC films.

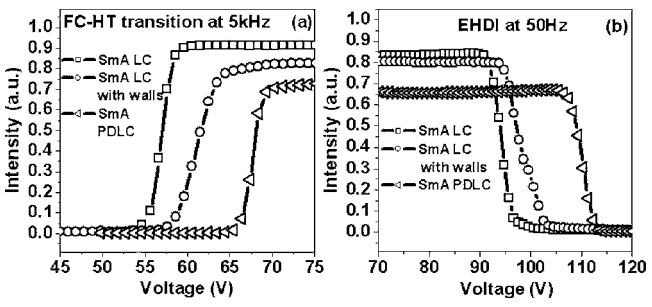

FIG. 2. The static-response curves for pure SmA LC, SmA LC with polymer walls, and SmA PDLC cells for EHDI and FC-HT transitions at (a) 5 kHz and (b) 50 Hz, respectively.

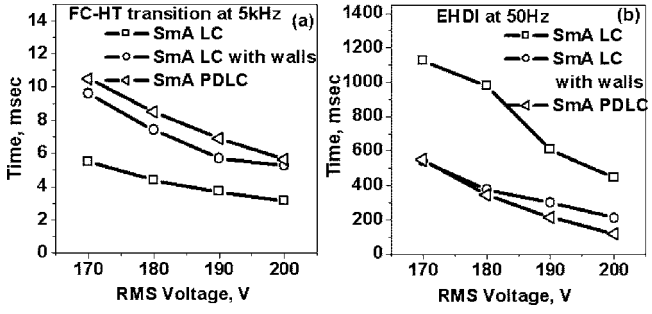

FIG. 3. Response times-voltage dependencies for pure SmA LC, SmA LC with polymer walls, and SmA PDLC cells for EHDI and FC-HT transitions at (a) 5 kHz and (b) 50 Hz, respectively.

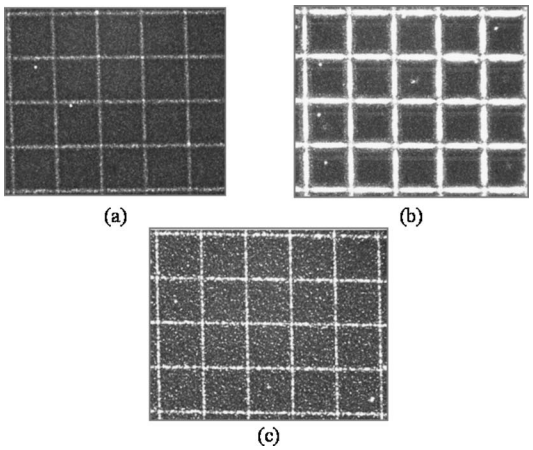

FIG. 4. Optical microscopy micrographs of (a) pure SmA LC, (b) SmA LC with polymer walls, and (c) SmA PDLC in a focal conic state with 5× magnification.

The transmission microscope micrographs of all the SmA cells in their scattering states are shown in Fig. 4. As seen in Fig. 4, we observed light leakage through the transparent polymer walls formed in the interpixel regions. However, in a real display the interpixel regions would be masked or a black background used. In such a case, the only thing that matter is how well the pixel areas scatter the light. Therefore, the CR values were determined by analyzing the transmission optical microscopy pictures of each pixel.

Keeping constant the illumination and the magnification of a Nikon transmission microscope, images of both the scattering and the clear states were computer digitized. We defined the pixel CR as the ratio of the average gray level for the clear state to the average gray level for the scattering state. CR data for all pixels shown in the transmission microscope micrographs were normalized and the CR results are tabulated in Table II. We found that the CR value of the polymer wall encapsulated SmA cell was 92.9% of that of the pure material on glass substrates, while the CR value for the PDLC system is 85.6%.

Compared with the PDLC system, both the clear and the scattering state are better for the SmA and for the encapsulated SmA, because the pixels are occupied mostly by the liquid crystal. The ordinary refractive index of the liquid crystal (n_o=1.51) and the refractive index of the polymer (n_p=1.52) are not mismatched. In contrast, such a slight mismatch is always apparent in the PDLC system. In addition, at an interface, the LC molecules do not switch as do the molecules in the bulk due to the strong anchoring forces. As a result, there is a residual transparency or scattering intrinsic to the PDLC system.

In Fig. 5, all three cells were photographed in their transparent states proving that the inclusion of polymer content out of pixel areas improves the transparency of SmA LC cells compared to the transparent state of PDLC. Overall, we found that SmA LC with polymer walls performed very similar to pure SmA LC, but better compared to the SmA PDLC cell.

TABLE II. The contrast ratios of SmA LC, SmA LC with polymer walls, and SmA PDLC cells.

Sample	CR	% CR
SmA LC mixture	3.59	100
SmA LC with polymer walls	3.34	92.9
SmA PDLC	3.08	85.6

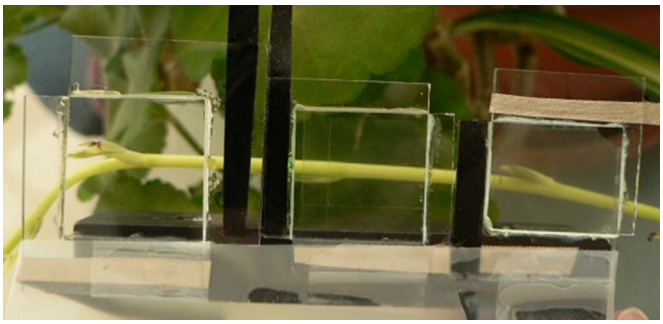

FIG. 5. (Color online) Pictures of pure SmA LC, SmA LC with polymer walls, and SmA PDLC in their transparent states on 0.75×0.75 in.^{2} sized glass substrates from left to right. No voltage is applied to maintain optical states.

In conclusion, we developed a composite system for use in order to produce robust bistable SmA LC based flexible displays by encapsulating the LC material between polymer walls. We demonstrated that both electro-optic response characteristics and contrast ratio values of SmA LC with polymer walls are very close to those of pure LC material. Our results confirmed that the developed technology can produce rugged and optically well performing bistable SmA LC devices. These prototypes on glass substrates show the potential use of polymer walls for low-cost realization of lightweight and bistable flexible LC display applications.

The authors would like to thank Liou Qiu of LCI, Kent State University for the SEM characterization of our liquid crystal films. The authors also thank Bentley Wall of LCI, Kent State University for his help throughout this project.

[1] D. K. Yang, J. L. West, L. C. Chien, and J. W. Doane, J. Appl. Phys. **76**, 1331 (1994).
[2] I. Dozov, M. Nobili, and G. Durand, Appl. Phys. Lett. **70**, 1179 (1997).
[3] G. P. Brown, SID Int. Symp. Digest Tech. Papers **31**, 76 (2000).
[4] Y. Ji, J. Francl, W. J. Fritz, P. J. Bos, and J. L. West, SID Int. Symp. Digest Tech. Papers **27**, 611 (1996).
[5] Y. Kim, J. J. Francl, B. Taheri, and J. L. West, Appl. Phys. Lett. **72**, 2253 (1998).
[6] J. L. West, G. R. Novotny, M. R. Fisch, and D. Heinman, Proc. IMID '01 Digest 3–6 (2001).
[7] W. A. Crossland and S. Canter, SID Int. Symp. Digest Tech. Papers **16**, 124 (1985).
[8] V. L. Aristov, M. V. Mitrokhin, V. P. Sevostyanov, and M. G. Tomilin, J. Opt. Technol. **65**, 573 (1998).
[9] M. V. Mitrokhin and B. Holter, SID Int. Symp. Digest Tech. Papers **36**, 1774 (2005).
[10] E. A. Buyuktanir, M. Mitrokhin, B. Holter, A. Glushchenko, and J. L. West, Jpn. J. Appl. Phys., Part 1 **45**, 4146 (2006).
[11] J. L. West, Mol. Cryst. Liq. Cryst. **157**, 427 (1988).
[12] E. A. Buyuktanir, A. Glushchenko, B. Wall, J. L. West, M. Mitrokhin, and B. Holter, SID Int. Symp. Digest Tech. Papers **36**, 1779 (2005).
[13] V. H. Bodnar, Y. Kim, B. Taheri, and J. L. West, Mol. Cryst. Liq. Cryst. Sci. Technol., Sect. A **329**, 405 (1999).
[14] J. D. Jackson, *Classical Electrodynamics*, 3rd ed. (Wiley, New York, 1999).